Pharmaceutical Research, Vol. 23, No. 10, October 2006 (© 2006)
DOI: 10.1007/s11095-006-9095-1

Research Paper

Rapid Assessment of the Structural Relaxation Behavior of Amorphous Pharmaceutical Solids: Effect of Residual Water on Molecular Mobility

Danforth P. Miller[1,2] and David Lechuga-Ballesteros[1]

Received January 26, 2006; accepted June 22, 2006; published online September 6, 2006

Purpose. Use RH-perfusion microcalorimetry and other analytical techniques to measure the interactions between water vapor and amorphous pharmaceutical solids; use these measurements and a mathematical model to provide a mechanistic understanding of observed calorimetric events.
Materials. Isothermal microcalorimetry was used to characterize interactions of water vapor with a model amorphous system, spray-dried raffinose. Differential scanning calorimetry was used to measure glass transition temperature, T_g. High-sensitivity differential scanning calorimetry was used to measure enthalpy relaxation. X-ray powder diffraction (XRPD) was used to confirm that the spray-dried samples were amorphous. Scanning electron microscopy (SEM) was used to examine particle morphology. Gravimetric vapor sorption was used to measure moisture sorption isotherms. Thermogravimetric analysis (TGA) was used to measure loss on drying.
Results. A moisture-induced thermal activity trace (MITAT) provides a rapid measure of the dependence of molecular mobility on moisture content at a given storage temperature. At some relative humidity threshold, RH_m, the MITAT exhibits a dramatic increase in the calorimetric rate of heat flux. Simulations using calorimetric data indicate that this thermal event is a consequence of enthalpy relaxation.
Conclusions. RH-perfusion microcalorimetry is a useful tool to determine the onset of moisture-induced physical instability of glassy pharmaceuticals and could find a broad application to determine appropriate storage conditions to ensure long-term physical stability. Remarkably, thermal events measured on practical laboratory timescales (hours to days) are relevant to the stability of amorphous materials on much longer, pharmaceutically relevant timescales (years). The mechanistic understanding of these observations in terms of enthalpy relaxation has added further value to the use of RH-perfusion calorimetry as a rapid means to characterize the molecular mobility of amorphous solids.

KEY WORDS: amorphous; enthalpy relaxation; glass transition temperature; hydration limit; microcalorimetry; MITAT; structural relaxation.

INTRODUCTION

The metastable nature of amorphous pharmaceutical solids is well known. Despite this challenge to their development into products, the improvement in key pharmaceutical properties of an amorphous drug could provide significant advantages. In many cases, this enables products that might not otherwise be developed. For example, the apparent solubility and/or dissolution rate of a crystalline drug with poor aqueous solubility can be improved by formulating and processing it to produce an amorphous solid. Also, many therapeutic proteins have greater physical and chemical stability when formulated in molecular dispersions with certain amorphous excipients. Though an amorphous drug product is sometimes deliberately developed, oftentimes, amorphous material is unintentionally produced during processing (e.g., during milling, precipitation from solution, compaction, lyophilization, etc.). Regardless of intent, the greater molecular mobility (relative to the crystalline state) of amorphous material could lead to physical events (i.e., collapse, crystallization) that adversely affect mechanical and morphological properties, which could ultimately impact product performance. Furthermore, chemical stability is often controlled by molecular mobility. Thus, a key challenge in the development of a partially or fully amorphous formulation lies in the ability to ensure that the formulation has acceptable long-term stability under pharmaceutically relevant storage conditions. Because of the cost and time necessary to conduct long-term stability studies, improving the ability to predict long-term chemical and physical stability has been an active area of research in our and others' laboratories.

In many cases, long-term stability is often synonymous with low "molecular mobility." For diffusion-controlled chemical reactions, translational and/or rotational molecular

[1] Nektar Therapeutics, 150 Industrial Road, San Carlos, California 94070, USA.
[2] To whom correspondence should be addressed. (e-mail: dmiller@nektar.com

mobility often determines chemical degradation rates. Because water vapor or residual moisture is often present during manufacture, storage, and use of pharmaceutical solids, there is a need to experimentally identify temperature and humidity conditions under which relaxation times (i.e., the time scale for long-range molecular motion) of an amorphous solid exceed the expected storage time. Several analytical methods [e.g., DSC (1), dielectric resonance spectroscopy (2), thermally stimulated depolarization current (3), NMR (4), isothermal microcalorimetry (5), and dynamic mechanical analysis (6)] have been used to estimate characteristic relaxation times. However, most studies involve assessment of the molecular mobility of dried materials (i.e., at or near zero water content); until recently, few studies have provided information on the effect of water content on characteristic relaxation times (7–10).

In a previous paper, we reported on the use of water vapor-perfusion or "RH-perfusion" microcalorimetry to measure interactions between water and amorphous materials (11). For a given amorphous material, this analytical technique was used to produce the moisture-induced thermal activity trace, abbreviated here as "MITAT." This plot of the thermal or calorimetric power as a function of relative humidity is a measure of the total, non-specific rate of heat flux due to interactions between a solid sample and water vapor. Figure 1 shows the MITAT of spray-dried (amorphous) raffinose at 25°C. The ordinate axis is referred to as calorimetric or thermal power, and is proportional to the rate of production or absorption of heat. In these experiments, exothermic thermal events are expressed as positive values.

The MITATs of many amorphous materials exhibit common features. For raffinose (see Fig. 1), there is a low activity region below 20% RH, a "take-off" point at about 20% RH, followed by a region of high exothermic activity between 20 and 40% RH. In this work, we designate this peak as the "α-peak." Similar behavior has been observed for other amorphous materials, including synthetic polymers, proteins, and hydrophilic and hydrophobic drugs (see Fig. 2).

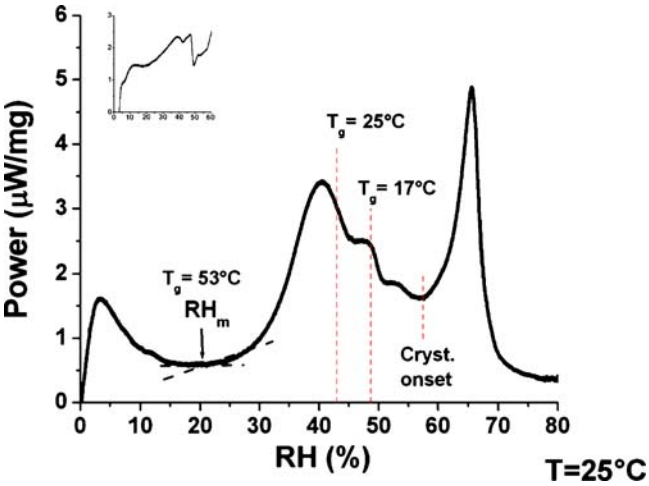

Fig. 1. Moisture-induced thermal activity trace of spray-dried raffinose (25°C). The indicated T_g values are based on a cubic spline interpolation of T_g(RH) data. *Inset*: MITAT trace for an experiment in which the RH ramp began at 3.5% RH to avoid artifact introduced at low RH (see text for details).

The so-called take-off point of a given amorphous material, RH_m, is assigned as the extrapolated onset of the α-peak, and is assessed using the intersections of lines drawn tangent to the calorimetric trace before and after the onset of this peak. The take-off point is of particular interest because it correlates with long-term physical stability. For example, the take-off point of amorphous sucrose is 12% RH at 25°C. Makower and Dye (12) found that sucrose remained amorphous for more than 2 years when stored at or below this relative humidity. In contrast, sucrose began to recrystallize within 200 days when stored at a slightly higher relative humidity, 16% RH. Based on this observation and experience with the development of amorphous formulations in our laboratories, RH-perfusion microcalorimetry has already proved to be a useful tool to quickly assess conditions that ensure physical stability over pharmaceutically relevant storage times.

In addition to a useful correlation between physical stability and RH_m, in previous work, we noted the correlation between the water sorption (BET) monolayer and RH_m. This so-called "monolayer" is the origin of the subscript used to describe the take-off point. One objective of this work is to further investigate these and other correlations to elucidate the underlying physical phenomenon that gives rise to a take-off point.

In one sense, RH-perfusion microcalorimetry can be considered as the relative humidity analog of differential scanning calorimetry (DSC). Whereas DSC is used to monitor a sample's energetic response to an imposed heating profile ("temperature scanning"), RH-perfusion microcalorimetry monitors the response of a material to a changing RH or residual water content. Because temperature is often a critical parameter for the processing, handling, and storage of a pharmaceutical product, DSC is a widely used characterization tool. Its widespread acceptance is a result of considerable efforts to understand and interpret observed thermal events, often using orthogonal analytical techniques (e.g., spectroscopy, X-ray powder diffraction, hot-stage microscopy). In contrast, despite the relevance of relative humidity conditions and residual water to the long-term stability of pharmaceutical solids, a review of the literature shows that RH perfusion calorimetry has only found limited use in the pharmaceutical and food science fields (13–15). This is in part due to the difficulties in interpreting thermal events induced by interactions of water vapor with a sample, which becomes especially challenging when the composition of the sample continuously changes during water vapor sorption or desorption.

Calorimetry is an extremely versatile analytical technique because all processes result in the absorption or production of heat. However, its non-specific nature makes it challenging to interpret and understand the origin of thermal events. The present study describes more recent work in our laboratories to add specificity and to quantitatively understand the key thermal events observed in the moisture-induced thermal activity traces of many amorphous materials. In this work, we used several other analytical techniques, including mathematical modeling, to elucidate the origin of the thermal events of the MITAT of a model amorphous material. Furthermore, we show the relevance of thermal events measured on practical laboratory timescales

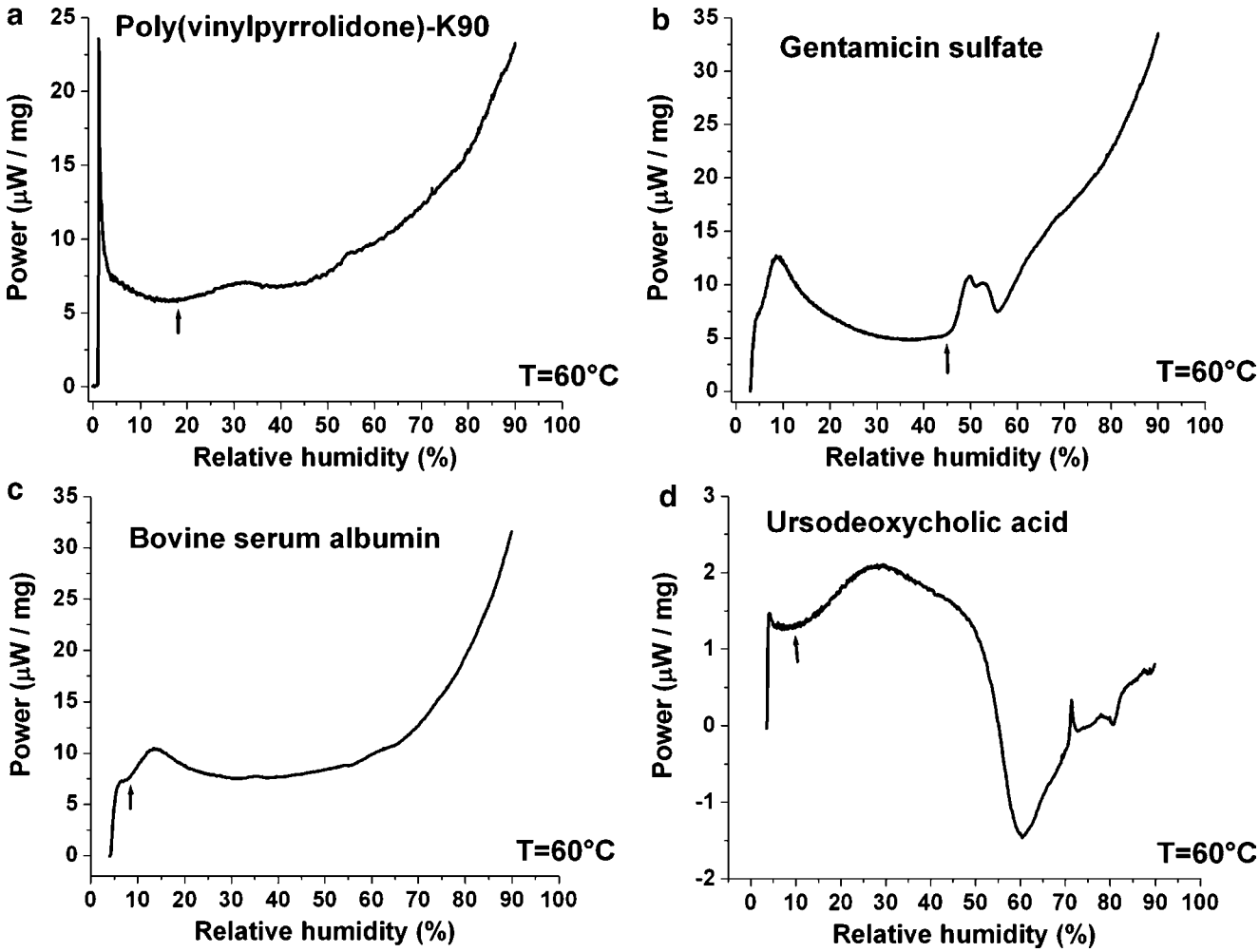

Fig. 2. The moisture induced thermal activity traces (MITAT) of several amorphous materials at 60°C. From *top* to *bottom*: PVP (raw material, as received), spray-dried gentamicin sulfate, spray-dried bovine serum albumin, and cryogenically milled ursodeoxycholic acid. *Arrows* indicate estimated RH_m values. All MITATs measured at a 6% RH/h scan rate, except for gentamicin sulfate (measured at 3% RH/h).

(hours to days) to the stability of amorphous materials on pharmaceutically relevant timescales (years).

MATERIALS

Raffinose pentahydrate was obtained from Ferro-Pfanstiehl (Waukegan, IL). Polyvinylpyrrolidone (PVP) K-90 was obtained from Fluka. Gentamicin sulfate was obtained from Long March Pharmaceuticals (China). Ursodeoxycholic acid and bovine serum albumin (Fraction V) were obtained from Sigma. All chemicals were of 99% purity or better.

To prepare amorphous raffinose, an aqueous solution of 2.0 wt.% solids content was spray-dried using a modified Büchi 190 spray-dryer. The (controlled) inlet and (measured) outlet gas temperatures were 120 and 75°C, respectively. To reduce structural relaxation of the amorphous powder during spray drying, the collector was cooled using a water bath at ambient temperature (about 20°C). Powder was stored in a drybox and handled in a glovebox at less than 3% RH at ambient temperature. Spray-dried gentamicin sulfate was prepared and handled in a similar manner, except the inlet and outlet gas temperatures were 125 and 80°C, respectively. Wide-angle X-ray powder diffraction was used to confirm that both spray-dried powders were amorphous.

To prepare amorphous ursodeoxycholic acid, a powder sample was cryogenically milled using a Spex SamplePrep 6750 Freezer/Mill. Approximately 1.8 g of crystalline powder were enclosed in a tube containing a magnetic impactor bar. The sample tube was immersed in liquid nitrogen and pre-cooled for 10 min, and then milled for 80 cycles, with each cycle consisting of alternating 1-min milling and 1-min resting (to dissipate heat) periods. The impactor bar shuttled along the length of the tube at a frequency of 10 Hz, which is equivalent to 20 impacts per second. Wide-angle X-ray powder diffraction was used to confirm that the milled powder was amorphous.

EX SITU RH EQUILIBRATION OF POWDER

To pre-equilibrate powder at discrete RH values, samples in open vials were stored in the vapor headspace of saturated salt solutions in vacuum desiccators, which were placed in a temperature-controlled incubator at 25°C (VWR, Model

1915). Each of the following salt solutions was used to provide an environment of a given relative humidity at 25°C (16): LiBr (6.4% RH), LiCl (11.3% RH), LiI (17.6% RH), $KC_2H_3O_2$ (22.5% RH), $MgCl_2$ (32.8% RH), K_2CO_3 (43.2% RH), $Mg(NO_3)_2$ (52.9% RH), NaBr (57.6% RH), $CoCl_2$ (64.9% RH), and NaCl (75.3% RH). All salts used were of 99% purity or better.

ISOTHERMAL MICROCALORIMETRY

The interactions of water with spray-dried amorphous raffinose were studied using a heat-conduction isothermal microcalorimetric system, Thermal Activity Monitor (TAM) Model 2277 (Thermometric AB, Sweden). At a given temperature, this technique measures the heat flux, P (typically measured in μW), or thermal power due to all energetic events. In each experiment, a powder sample was placed into a stainless steel ampoule and connected to a Gas Pressure Controller Device (GPCD) (Model 2255-120 Thermometric AB, Sweden) that accurately controls the relative humidity (RH) within the measurement ampoule (0 to 90 ± 0.1% RH) as a step function or a linear ramp (17). An empty, closed ampoule was used as a reference cell. Dry N_2 was used as the carrier gas at a constant flow rate (160 standard cm^3/h). The relative humidity was controlled by splitting the total flow of the carrier gas into two streams. One stream was fed directly to the sample ampoule, (i.e., the "dry stream"), while the other ("wet") stream was fed to two successive humidification chambers. A stream of a given relative humidity was then produced by controlling the ratio of the flow rates of the wet and dry streams using mass flow controllers. This method requires a mathematical correction to the relative humidity in order to account for the increase in mass flow rate as the nitrogen stream passes through the humidification chambers. This correction was used throughout this work.

In the RH-perfusion experiments of this work, an amorphous sample was exposed to a vapor stream of continuously increasing RH. About 10 to 15 mg of powder were placed into a stainless steel ampoule and dried *in situ* by flowing a dry nitrogen stream (≈0% RH) until there was no measurable thermal activity (i.e., P was within the range from −1 to +1 μW). The RH was then increased in a linear ramp from 0 to 90% RH over the following 30 h (i.e., at 3% RH/h). In some cases, RH scans were started at some low, non-zero RH in order to avoid an artifact introduced by the mass flow controllers used to control RH (discussed later). The heat flow resulting from the moisture interaction with the solid sample was measured as a function of time. An identical experiment was performed using an empty ampoule. This background contribution was subtracted from all data reported here.

MODULATED DIFFERENTIAL SCANNING CALORIMETRY

The glass transition temperature, T_g, of a given sample was measured using a TA Instruments Model Q1000 differential scanning calorimeter equipped with a refrigerated cooling system (New Castle, Delaware). The sample cell was purged with dry nitrogen at a flow rate of 50 cm^3/min. Aluminum pans that contained between 2 and 10 mg of powder were hermetically sealed. For an open-pan modulated DSC experiment, the lid of the pan was pierced just prior to the run. The scans were performed at a heating rate of 2°C/min and a modulation amplitude and period of ±0.318°C and 60 s, respectively. These modulation conditions result in a "heat only" modulation cycle. Each reported T_g corresponds to the extrapolated onset of the transition.

HIGH SENSITIVITY DIFFERENTIAL SCANNING CALORIMETRY

Isothermal enthalpy relaxation experiments were conducted using a Setaram Micro DSC III (Setaram Inc., Caluire, France). Prior to an experiment, each powder sample was pre-equilibrated at a given RH for several days and then sealed into a 0.85 cm^3 stainless steel ampoule. To reduce the effect of moisture redistribution between the powder and the headspace in the ampoule, the headspace volume was minimized by tamping the powder so that approximately 300–800 mg powder fit into the ampoule. In the worst-case scenario (i.e., the highest temperature experiment), calculations show that approximately 0.014 mg water would evaporate into the ampoule headspace, resulting in a water content change of less than 0.01 wt.% H_2O. The enthalpy associated with moisture equilibration would be less than 50 mJ. Thus, these experiments can be assumed to occur at nearly constant water content (though, due to the temperature-dependence of moisture sorption isotherms, the equilibrium RH inside the ampoule will depend on the temperature).

The thermal history of each amorphous sample was controlled by heating at 1°C/min to 10°C above T_g and then cooling at the same rate to an aging temperature (below T_g) at which enthalpy relaxation was monitored for 24 h. To reduce the effects of moisture redistribution and the presence of temperature gradients across the sample during establishment of thermal equilibrium, the first 10 min of data were ignored in the analysis of isothermal enthalpy relaxation. Relaxation or "isothermal aging" measurements were performed at several temperatures on a single sample with a given water content. Between isothermal aging experiments, the thermal history of the sample was erased by reheating the sample at 1°C/min to 10°C above T_g, and then cooling at the same rate to the next aging temperature.

X-RAY POWDER DIFFRACTION

X-ray powder diffraction (XRPD) studies were performed using an XRD-6000 diffractometer (Shimadzu Corporation, Japan). Samples were scanned from 3 to 40°2θ, at 3°2θ/min, with a step size of 0.04°2θ, using a Cu radiation source with a wavelength of 1.54 Å operated at 45 kV and 30 mA. To control the RH above the powder sample, an Anton Paar TTK 450 (Austria) environmental chamber attachment was integrated with a VTI Corporation (Hialeah, Florida) RH-200 humidity generator.

WATER VAPOR SORPTION/DESORPTION

Gravimetric water vapor sorption/desorption studies were conducted with a DVS-1000 dynamic vapor sorption system (Surface Measurement Systems, UK). The powder samples (10 to 20 mg) were initially dried at 25°C until a constant weight was achieved. The relative humidity was then increased from 0 to 90% in increments of 5% RH. At each step, the RH was held constant until the rate of mass change (dm/dt) was less than the programmed equilibrium criterion, 0.001%/min. For a "ramp" experiment, the sample was dried in the same manner as above, and then it was exposed to a linear ramp in RH from 0 to 90% RH at 3% RH/h.

THERMOGRAVIMETRIC ANALYSIS

The weight loss upon drying was measured using a TA Instruments Model TGA-2950 Hi-Res instrument (New Castle, DE). A sample mass between 5 and 15 mg was used for each experiment. Each sample was heated from 25 to 110°C at 2°C/min. The temperature was then held at 110°C for at least 90 min. The weight loss upon drying was calculated using the initial sample mass and that at the end of the isothermal step.

SCANNING ELECTRON MICROSCOPY

Scanning electron microscopy (SEM) was used to observe the morphology of the spray-dried particles before and after exposure to moisture. Samples were mounted on silicon wafers that were then mounted on top of double-sided carbon tape on an aluminum SEM stub. The mounted powders were then sputter-coated with gold/palladium in a Denton sputter-coater for 60 to 90 s at 75 mTorr and 42 mA. This produces a coating thickness of approximately 150 Å. Images were taken with a Philips XL30 ESEM operated in high vacuum mode using an Everhart–Thornley detector to capture secondary electrons for the image composition. The accelerating voltage was set at 20 kV using a LaB_6 source. The working distance was between 5 and 6 mm.

DISCUSSION AND RESULTS

Throughout this work, results are most often interpreted and expressed in terms of RH rather than water content. This convention is used here because RH is the independent variable in RH-perfusion calorimetry, which is the focus of this work. Water content and RH are interconvertible; at a given temperature, a material's moisture sorption isotherm relates its water content to the RH. Though RH is most commonly a measure of a sample's environment (and water content is a measure of the sample itself), RH is also sometimes described as a sample property (e.g., the concept of water activity used in the food science literature). To support the use of either convention in this work, method development work was done to evaluate the differences between experiments on equilibrated samples (static measurements) and results from dynamic measurements in which the sample's composition (wt.% H_2O) and its environment (RH) change continuously.

RH-PERFUSION CALORIMETRY METHOD DEVELOPMENT

The previously mentioned analogy between RH-perfusion microcalorimetry and differential scanning calorimetry provides a useful basis of comparison for readers who are familiar with DSC. Whereas DSC is used to monitor the energetic response ("heat flow") to an imposed heating profile ("temperature scanning"), RH-perfusion microcalorimetry monitors the energetic response of a material to a changing RH. To ensure quasi-equilibrium conditions in a DSC experiment, the heating rate is limited by the thermal diffusivity of the sample material. In a similar fashion, in an RH-perfusion experiment, the diffusivity of water in the material places a limit on the maximum RH scan rate that can be used for a given sample size.

Because water uptake tends to be a diffusion-limited process, development of an RH-perfusion microcalorimetry method requires optimization of the following parameters: sample mass and geometry, RH ramp rate, and carrier gas flow rate. The equation relating these parameters to the cumulative mass of perfused water at a given relative humidity, $m(RH)$, is given by:

$$\frac{m(RH)}{m_s} = \frac{1}{m_s}\frac{P^{sat}(T)\dot{V}M}{100RT}\frac{(RH)^2}{2(\dot{RH})} \tag{1}$$

where $P^{sat}(T)$ is the vapor pressure of water at the experiment temperature, T, M is the molecular weight of water, R is the universal gas constant, $\dot{V}$ is the volumetric flow rate of the carrier gas, m_s is the sample mass, and $\dot{RH}$ is the rate at which relative humidity is linearly increased. To ensure "sink" conditions within the calorimetric ampoule, the incoming gas stream must supply an excess of water relative to that adsorbed or absorbed. Based on the above equation, the preferred combination of parameters would be the use of a small sample, a high carrier gas flow rate, and a low RH ramp rate. However, a sufficiently large sample must be used to provide an acceptable signal to noise ratio. Also, the design of the gas pressure controller device (GPCD) limits the carrier gas flow rate. Because one of the incoming carrier gas streams is saturated with water by passing it through the hydrator vessels of the calorimetric flow cell, a sufficiently low flow rate of the carrier gas must be selected to ensure an adequate contact time between the carrier gas and the water in the hydrator vessels. Practical considerations around the duration of the experiment place a lower bound on the RH ramp rate. Furthermore, at high temperatures, low RH ramp rates may not be possible because of depletion of the water in the hydration vessels during a long (weeks) experiment.

When interpreting results measured using dynamic techniques (RH-scanning experiments in either gravimetric vapor sorption or RH-perfusion calorimetry experiments, or temperature-scanning DSC experiments), it is emphasized that the sample in each of these techniques is in quasi-equilibrium. For RH-perfusion calorimetry experiments, method development is necessary to optimize experiment parameters and to assess the extent of deviation from equilibrium when using those parameters.

A statistical design of experiments was conducted to determine the optimum sample mass, RH ramp rate, and

carrier gas flow rate. The approach to equilibrium was assessed by comparison of the results of two types of experiments. First, a spray-dried PVP-K90 sample was exposed to an RH ramp from 0 to 20% RH (at 25°C), and the total integrated heat was determined for this RH range. In the second type of experiment, the total integrated heat was determined when the RH was increased to 20% RH in a single step and sufficient time was allowed for sorption to proceed to completion. In the stepwise experiment, the sample is assumed to be in moisture sorption equilibrium, and the absolute value of the integrated heat represents the maximum possible value for any ramp experiment.

For method development purposes, this material and RH range was chosen to ensure that all heat effects were due only to moisture sorption—i.e., because PVP was well below its T_g at all RH values, all events were energetically reversible. Spray-dried PVP was also selected because it would be expected to be similar to other amorphous systems with respect to its hygroscopicity, specific surface area, and the diffusivity of water within the solid. Based on the RH ramp method used here, the integrated heat from the ramp experiment (3% RH/h) was 94% of that from the RH-step experiment, indicating that quasi-equilibrium conditions were attained. In comparison, for spray-dried raffinose, the integrated enthalpy from the ramp experiment (3% RH/h) was 95% of that from the RH-step experiment. Thus, the method used here provides a high flow rate of carrier gas, a modest RH ramp rate, and a sufficiently low sample mass, yet enough sample material to ensure a suitable signal to noise ratio.

Though the above approach reduces the departure from equilibrium moisture sorption, it does not eliminate it. To assess a material under static conditions, one approach is to conduct experiments at several RH scan rates and then extrapolate results to zero scan rate. Because of the weak dependence of results on RH scan rate and because the signal to noise ratio suffers when using very low scan rates, this extrapolation approach was not used in this work.

RAFFINOSE AS A MODEL SYSTEM

For much of the work of this study, raffinose was selected as a model amorphous material for several reasons. First, this trisaccharide readily forms an amorphous solid upon spray-drying and has a sufficiently high glass transition temperature, T_g, to enable studies over a broad RH range (or range of water content). Second, raffinose remains amorphous following exposure to moderately humid conditions, including those that depress the T_g of the hydrated raffinose below ambient conditions. This enables "erasure" of its thermal history (by scanning to temperatures above T_g) without the risk of crystallization. Finally, from work in our own and others' laboratories (18–20) there is a substantial amount of fundamental physicochemical data for this compound.

Figure 3 shows the T_g and water content of raffinose as a function of RH. Here, water contents were determined using two different techniques. The moisture sorption isotherm was determined using gravimetric vapor sorption. Also, the moisture contents of powder samples equilibrated (for at least 1 week) at several RH values were determined based on the loss on drying measured using thermogravimetric analysis. The good agreement between the results of these techniques indicates that the (dynamic) gravimetric moisture sorption experiments were conducted over a sufficient timescale to ensure attainment of equilibrium moisture sorption.

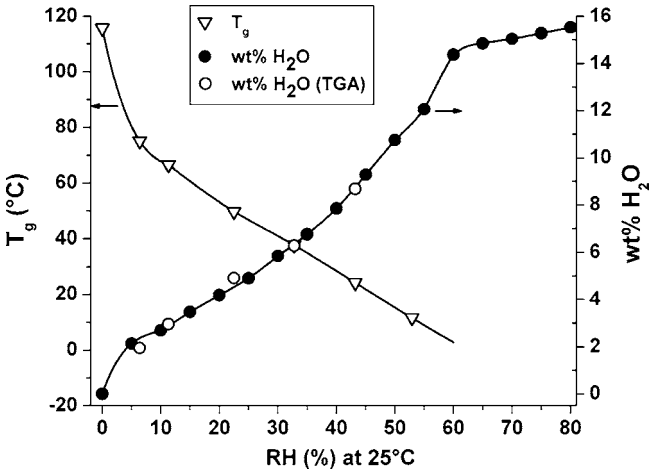

Fig. 3. Calorimetric glass transition temperature and water content of spray-dried raffinose as a function of relative humidity (25°C). Water content was determined using gravimetric vapor sorption. Loss on drying results, as determined from loss on drying measurements using thermogravimetric analysis, for discrete samples equilibrated at various RH values are provided for comparison.

From Fig. 3, the calorimetric T_g of dry raffinose is about 116°C (heating at 2°C/min); upon sorption of water vapor, T_g decreases to ambient temperature (25°C) at about 43% RH (see Fig. 3). Because its stable crystalline form, raffinose pentahydrate, contains 15.2 wt.% H_2O, recrystallization from the amorphous state is retarded below this water content. Figure 4 shows the X-ray powder diffraction patterns of raffinose following long-term exposure to several RH values at 25°C; the onset of recrystallization is detected at 53% RH, at which T_g = 11°C. This RH is consistent with a water content of about 11.5 wt.% H_2O. Crystallization at this overall water content, a lower water than that of raffinose pentahydrate, could be due to a gradient in moisture content incurred during exposure of the samples to water vapor. That is, surface material could have experienced a higher local water content, leading to crystallization.

In a DSC experiment to measure T_g, the temperature is increased at a constant rate. In contrast, in an RH-perfusion experiment, the temperature is constant and the T_g of the sample continuously decreases from its initial, "dry" value as RH is increased. The MITAT of raffinose contains several qualitative features that are also observed for many other amorphous materials. First, at 0 to 5% RH, there is a shoulder with a superimposed peak due to the onset of moisture sorption. Much of this initial peak is an artifact of the experimental apparatus; at 0 to about 3% RH, the mass flow controller for the humid gas stream is unable to deliver gas at extremely low flow rates. As the RH setpoint increases slightly (above 3% RH), the mass flow controllers resume the ability to accurately deliver the gas streams in the correct proportions. The high thermal activity is due to the sudden "burst" in water vapor delivered to the sample and pressure-volume work (due to the sudden increase in overall mass flow

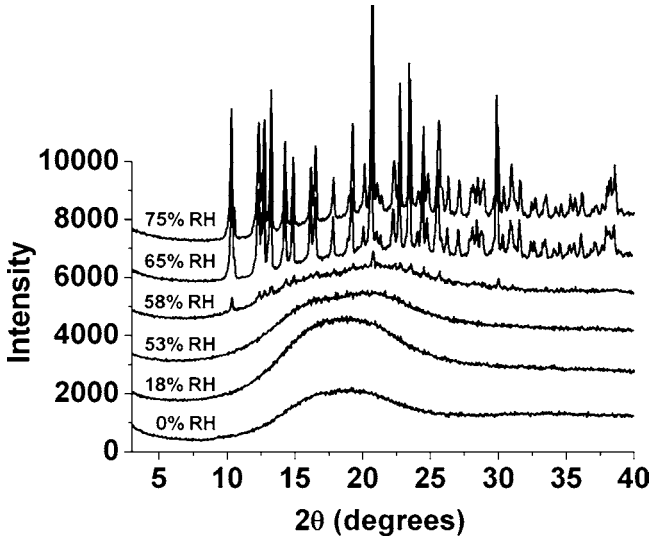

Fig. 4. X-ray powder diffraction patterns of spray-dried raffinose following exposure to the given relative humidities (at 25°C) for more than 8 weeks. Traces are vertically offset for clarity.

rate). This hypothesis has been tested by using a previous version of the RH-perfusion apparatus that instead uses a flow switch to control the proportions of the dry and "wet" gas streams. In that case (not shown), the thermal power at low RH rises much more slowly. To avoid this artifact when using mass flow controllers, RH ramp experiments of other experiments have been started at a modest RH (e.g., 3% RH), though this results in loss of continuous data at lower RH values (see inset of Fig. 1).

Interpretation of the thermal events the MITAT trace requires knowledge of the glass transition temperature as a function of RH. To this end, the MITAT in Fig. 1 has been annotated with T_g(RH) data. The take-off point or onset RH, RH_m, of spray-dried raffinose is determined by the intersection of the linear extrapolation of the baseline prior to the exothermic peak ("α-peak") and the line tangent to the front of the peak. The take-off point of raffinose occurs at about 20% RH. For an experiment conducted at 25°C, raffinose is 28°C below its T_g at this RH (see Fig. 3).

As RH is increased beyond RH_m, a broad, exothermic peak ("α-peak") occurs. At an RH slightly beyond the peak maximum, the thermal power "levels off" at a local minimum. As RH is increased further, there is a sudden decrease in thermal power. Materials that crystallize will exhibit another peak, the sign (i.e., endothermic or exothermic) of which depends on whether an anhydrous or hydrated crystal forms and whether water vapor is absorbed or liberated upon crystallization. Materials that do not crystallize (e.g., many synthetic polymers and proteins) will continue to adsorb and/or absorb water at increasing rates (and increasing thermal power).

Because sorption is highly energetic and will contribute greatly to the MITAT, it is desirable to know whether the take-off point is related to a change in the rate of moisture sorption. In a separate approach to decouple the thermal events due to moisture sorption from those due to other energetic processes, the rate of moisture sorption was gravimetrically measured using a gravimetric vapor sorption instrument (using the same RH ramp rate used in the calorimetric experiment). To enable comparison with RH-perfusion data, the rate of moisture sorption was calculated from the first derivative of the water uptake *versus* time data. Figure 5 shows a comparison of the time derivative of the water uptake data and the calorimetric (MITAT) results. Though, due to its increased sensitivity, the calorimetric profile has less noise, the derivative (gravimetric) data exhibits some features that are qualitatively similar to those in the MITAT.

For example, at about 47% RH, the MITAT and gravimetric (dm/dt) data both exhibit a decrease in rate. Based on T_g(RH) data, the T_g at this RH is about 20°C. Other workers have shown that, when the T_g of an amorphous material decreases below the experiment temperature, viscous flow can occur, eventually leading to collapse (21,22). This has been proposed to occur when the material reaches a critical viscosity for flow to occur over the time scale of observation (23). For fine particles observed over several hours, the critical viscosity is about 10^9–10^{11} Pa s (24), which is typically attained when T_g decreases to 5 to 15°C below the measurement temperature. This is consistent with previous results from our laboratory (11)—the collapse of spray-dried raffinose particles, as determined by a decrease in specific surface area, begins to occur somewhere between 31 and 43% RH (at the latter RH, T_g = 25°C). SEM images (Fig. 6) show that raffinose remains as discrete particles following storage as high as 38% RH (25°C); gross moisture-induced physical changes occur at higher RH values. Thus, the reduction in specific surface area results in a decrease in the moisture sorption rate, as measured both calorimetrically and gravimetrically.

Despite their similarities, note that the gravimetric data neither exhibit a well-defined take-off point nor a peak profile similar to that observed in the MITAT. Thus, the calorimetric take-off point and α-peak are not *directly* related to the amount or rate of moisture sorption. Nevertheless, analysis of derivative gravimetric moisture uptake data does provide a useful means to detect the RH threshold that leads to macroscopic structural collapse of an amorphous material. This phenomenon alone is known to be a main failure mode

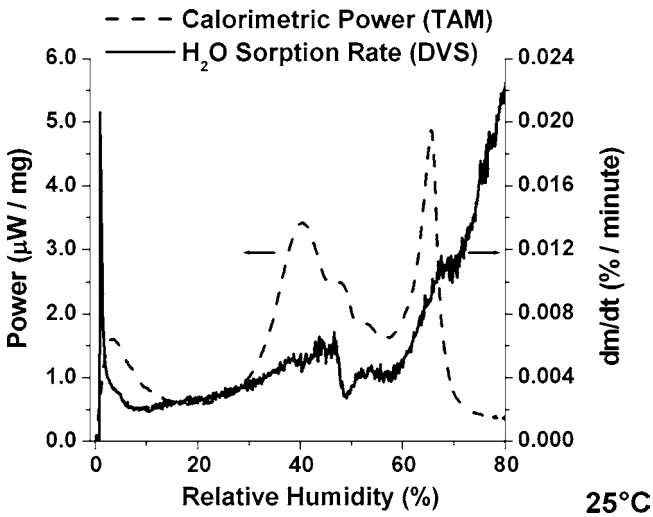

Fig. 5. Gravimetric (dm/dt; *solid trace*) and calorimetric (*dashed trace*) measurements during moisture uptake at 25°C as a function of RH. In both cases, RH was increased linearly at 3% RH/h. The spike in the gravimetric data at 0 to 5% RH is an artifact of the performance of mass flow controllers at low flow rates.

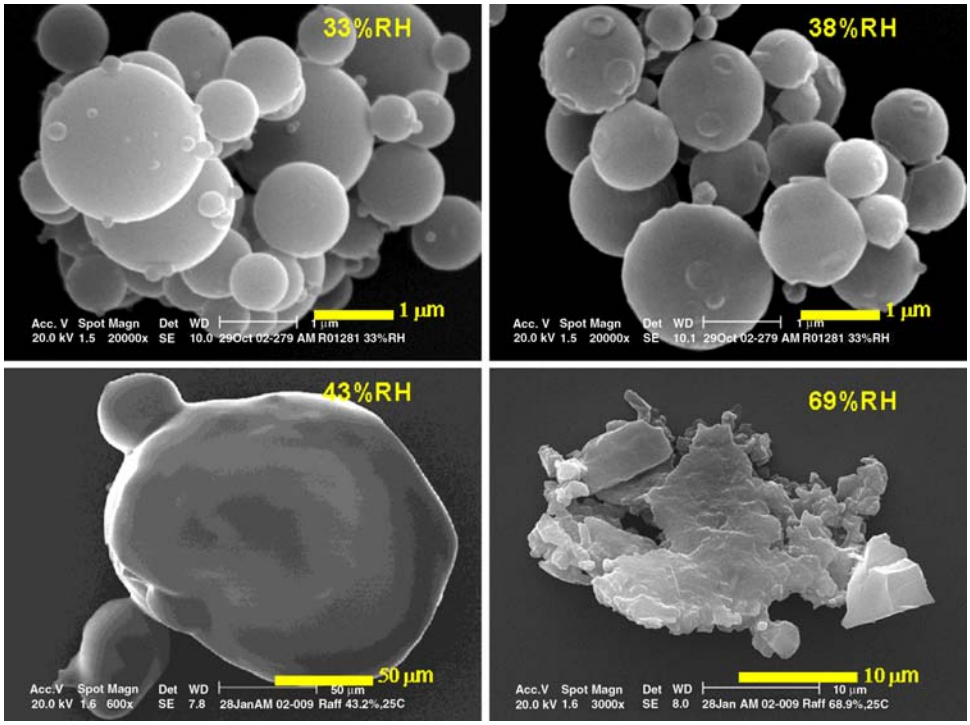

Fig. 6. SEM images of spray-dried raffinose following exposure to the given relative humidities (25°C) for more than 8 weeks. Raffinose remains as discrete, spherical particles following storage as high as 38% RH; at higher RH values (e.g., 43.2% RH), viscous flow results in bridging of particles. Recrystallization occurs at even higher RH values, as indicated by *angular features* in the image at 69% RH (as confirmed by X-ray powder diffraction results—see Fig. 4).

for amorphous food powders (25) and lyophilized protein formulations (2).

Labeling the MITAT with the T_g values measured using DSC facilitates interpretation of its key features. However, care must be taken when inferring the T_g of a sample in an RH-perfusion experiment based upon DSC measurements on samples pre-equilibrated at given RH values. These two analytical techniques do not measure the T_g over the same observation period (or at an equivalent frequency). If the width of a typical glass transition event is about 15°C for a sample heated at 2°C/min in a DSC experiment, then the period of observation is about 500 s. For an RH scan, however, the observation period is much longer. For example, in the region of T_g = 25°C (see Fig. 3) the T_g of raffinose decreases by about 15°C for every 10% increase of RH. For an RH scan rate of 3% RH/h, this RH change occurs over more than 3 h. Thus, the observation period for the RH-perfusion experiment is about 20 times greater than that for a DSC experiment at 2°C/min. Because of this difference, the estimated T_g from an RH perfusion experiment would be expected to be lower than that estimated from a DSC experiment. Hancock *et al.* (26) show the effect of DSC heating rate on the measured T_g of several amorphous solids; for each order of magnitude decrease in scanning rate, T_g decreased by about 7°C. Because the frequency dependence on T_g is slight (within a few degrees), and because the sample is in quasi equilibrium during an RH scan, these two effects will partially compensate one another, and the impact on our results will be minimal.

Inspection of Fig. 1 shows that the T_g of the plasticized raffinose at the end of the α-peak approaches the experimental temperature (25°C). This suggests that this peak is related to enthalpy relaxation (and only indirectly to moisture sorption), a phenomenon that occurs during storage at temperatures below T_g. Enthalpy relaxation occurs spontaneously for an amorphous material stored below its fictive temperature, the temperature of the (metastable) equilibrium supercooled glass with the same enthalpy as that of the real glass. Because the fictive temperature (based on enthalpy) of a freshly prepared sample is often within a few degrees (K) of T_g, we neglect the differences between the fictive temperature and T_g as we attempt to relate the observations of the MITAT with structural relaxation. Volume and enthalpy relaxation phenomena have been extensively studied, and for a more thorough explanation, the reader is directed to the physics, food science, materials science, mineralogy, and pharmaceutics literature [please see Hodge (27), Angell *et al.* (28), Moynihan (29), Struik (30), Liu *et al.* (5), Tool (31), Narayanaswamy (32), and McKenna (33)].

The relaxation function, ϕ, relates the time-dependent relaxation enthalpy, ΔH_r, to the enthalpy change to relax to the "equilibrium" glass, ΔH_r^∞ :

$$\phi = 1 - \frac{\Delta H_r}{\Delta H_r^\infty} \tag{2}$$

A relaxation model relates the rate of change of the relaxation function with time to more physically meaningful parameters. The Kohlrausch–Williams–Watts (KWW) stretched exponential function (34,35) has been used to model several molecular processes, among them, volume (30,36) enthalpy (37), and dielectric relaxation (35), protein

aggregation (38), and NMR data. The KWW equation is given by:

$$\phi = \exp\left(-\left(\frac{t}{\tau}\right)^{\beta}\right) \tag{3}$$

where τ is a characteristic relaxation time and β is the degree of non-exponentiality. This "stretching" parameter, β, is also considered to be a measure of the width of the distribution of Trelaxation times and the fragility of the glass; lower β values denote a broad distribution of relaxation times and a more fragile glass. For organic glass formers and mixtures thereof, typical β values are reported to be between 0.3 and 0.7 (39).

Note that there is no universally accepted model for relaxation processes-several other equations have been proposed [e.g., bi- and tri-exponential models (40), double KWW functions to model processes with slow and fast relaxation processes, the modified stretched exponential [MSE] Eq. (5)]. Because the KWW model is able to describe relaxation data for the materials of this study reasonably well, we chose it for its simplicity-most models use more adjustable parameters than the two parameters used in the KWW model.

To determine the contribution of enthalpy relaxation to thermal power, P, the differentiated form of the KWW equation is used (5):

$$P = \frac{d\phi}{dt} = \Delta H_r^{\infty} \frac{\beta}{\tau}\left(\frac{t}{\tau}\right)^{\beta-1} \exp\left(-\left(\frac{t}{\tau}\right)^{\beta}\right) \tag{4}$$

By assuming that the heat capacity difference between the glass and the supercooled liquid, ΔC_p, is independent of temperature and that the fictive temperature equals the glass transition temperature, ΔH_r^{∞} can be *estimated* using:

$$\Delta H_r^{\infty} \approx \Delta C_P \cdot \left(T_g - T\right) \tag{5}$$

Many workers have used enthalpy relaxation or enthalpy recovery measurements to probe molecular mobility in amorphous pharmaceutical solids stored below their T_g (1, 2, 5, 38). Enthalpy recovery measurements are commonly made using DSC or modulated DSC. Using DSC, the extent of enthalpy *recovery* is measured for samples aged for different times at a given storage temperature. To determine relaxation parameters, discrete values of recovered enthalpy *versus* time data are fit to a relaxation model. In recent years, isothermal microcalorimetry has enabled continuous monitoring of enthalpy relaxation (5). Besides the collection of more data points, the isothermal microcalorimetry approach allows determination of relaxation parameters from a single experiment (as compared to the multiple experiments required for a typical DSC-based method).

In this work, high-sensitivity DSC experiments were used to estimate relaxation parameters for samples of fixed composition (residual water content). This technique provides the advantages of both the DSC and isothermal microcalorimetric methods-high sensitivity to enable real-time monitoring of enthalpy relaxation, and the ability to scan temperature, which enables precise control of a sample's thermal history. The benefits (and disadvantages) of high-sensitivity DSC compared with other methods used to estimate relaxation parameters will be the subject of another paper.

To determine the effect of residual moisture on molecular mobility using high-sensitivity DSC, measurements were conducted on powders that were pre-equilibrated at various RH values (at 25°C). Figure 7 shows enthalpy relaxation data at several sub-T_g temperatures for a raffinose sample that had been pre-equilibrated to 22.5% RH (25°C). In such experiments, the calorimetric power (positive values indicate exothermic processes) is proportional to the rate of enthalpy relaxation, assuming that there are no other energetic processes that occur. As expected, the rate of enthalpy relaxation increases as the storage temperature approaches T_g. As previously noted, to reduce the contribution of transient effects (e.g., heat conduction, moisture re-equilibration), the first 10 min of each data set was ignored in the analysis of isothermal enthalpy relaxation data.

To estimate relaxation parameters, the Levenberg–Marquardt algorithm was used to perform a non-linear least squares minimization (Microcal Origin, version 6.0) of each set of relaxation data using the differential form of the KWW equation [Eq. (4)]. Convergence was improved when time was expressed in units of hours (rather than units of seconds used in data acquisition). Kawakami and Pikal (41) have noted that, because of opposite trends in the values of τ and β, τ^{β} tends to be less sensitive to curve fitting uncertainty than τ. We have also found this to be the case. Furthermore, as an amorphous material undergoes relaxation, τ increases and β tends to decrease. Kawakami and Pikal noted that these changes tend to offset one another, making τ^{β} a more "stable" parameter.

In recent years, such isothermal enthalpy relaxation measurements have become more routine in the development of stable amorphous pharmaceutical formulations. With some effort, the relaxation parameters of a given, fixed composition, can be determined at several temperatures of interest (37). In contrast, in an RH-perfusion experiment, the

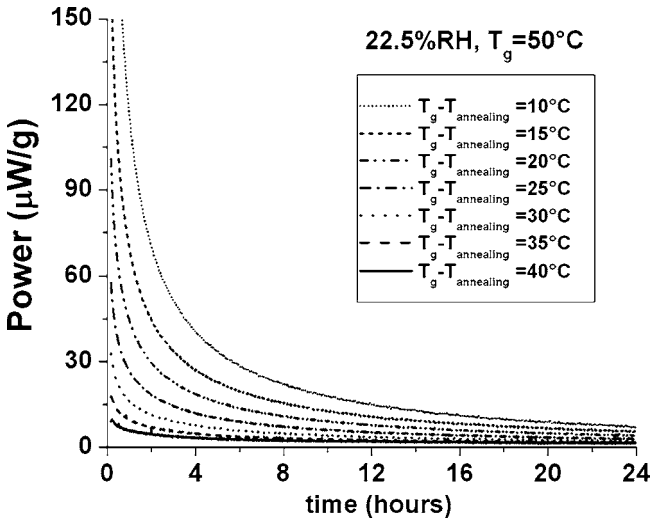

Fig. 7. Enthalpy relaxation of raffinose that has been equilibrated at 22.5% RH/25°C, as measured using high-sensitivity DSC (isothermal microcalorimetry). Calorimetric power was monitored for 24 h at seven annealing temperatures between 10 and 40°C below T_g. Annealing temperature decreases from *right* to *left*.

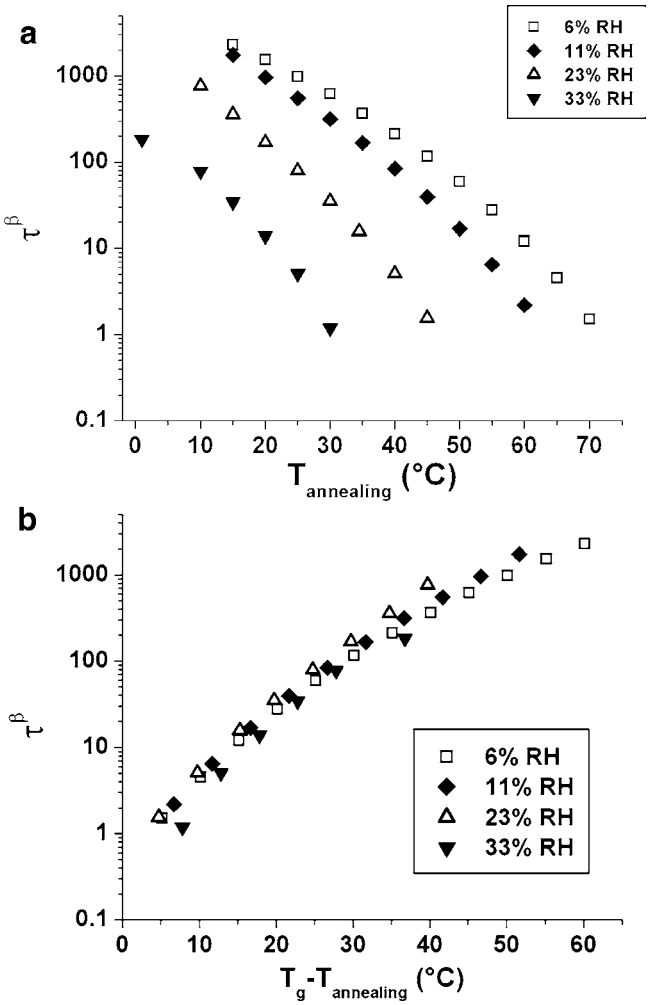

Fig. 8. Characteristic relaxation function, τ^{β}, of spray-dried raffinose as a function of (a) annealing temperature, or (b) temperature interval below the glass transition, $T_g - T$. In both cases, τ is expressed in units of days. Results for powders equilibrated at several RH values are shown (powders were RH-equilibrated at 25°C, aging experiments conducted at several temperatures). Relaxation parameters τ and β are based upon non-linear least squares fitting of enthalpy relaxation data to Eq. (4).

sample composition and T_g are changing in a non-linear manner with respect to time (or RH). Because of this complexity (and the non-exponentiality and non-linearity of enthalpy relaxation), it is difficult to envision the calorimetric manifestation of enthalpy relaxation as RH (and moisture content) continuously changes.

Figure 8 shows the results of fitting isothermal enthalpy relaxation data of raffinose to the differentiated form of the KWW equation [Eq. (4)]. These data represent the results of 36 separate 24-h isothermal relaxation experiments on amorphous raffinose equilibrated at 6.4, 11.3, 22.5, and 32.8% RH. Figure 8a shows the characteristic relaxation function, τ^{β}, of spray-dried raffinose as a function of annealing (or aging) temperature. At any temperature, the characteristic relaxation time increases as water content (or RH) is reduced, as expected. When expressed in terms of the storage temperature interval below T_g, $T_g - T$, this collection of points collapses to a narrow band (see Fig. 8b). This demonstrates that, over this range of water content (or RH), there is a superposition of the effects of moisture and temperature. That is, when expressed on the basis of the storage temperature interval below T_g, different hydrated raffinose samples exhibit similar relaxation behavior and this behavior is a strong function of $T_g - T$.

To visualize the contribution of enthalpy relaxation to the calorimetric power, [Eq. (4)] can be simplified for the special case in which the observation period is much shorter than the characteristic relaxation time, which occurs when relaxation has not occurred to any significant extent ($\phi \approx 1$), giving:

$$P \approx \Delta H_r^{\infty} \frac{\beta}{\tau} \left(\frac{t}{\tau}\right)^{\beta-1} \qquad (t << \tau) \qquad (6)$$

In this simplified case, the thermal power is proportional to β and the driving force for enthalpy relaxation, ΔH_r^{∞}, and inversely proportional to the characteristic relaxation time. These qualitative relationships will be critical to understanding the MITATs of raffinose and other amorphous solids.

The trends in these quantities (the driving force for relaxation and the relaxation rate) with RH can be estimated by interpolating results determined from experiments conducted at discrete RH values. Figure 9 shows that the estimated relaxation rate (given as the reciprocal of the characteristic relaxation time) at 25°C as a function of $T_g - T$. Comprehension of the conceptual basis of this figure is *essential* to understanding the origin of the take-off point and the associated α-peak of amorphous materials. At low RH, the driving force for enthalpy relaxation (ΔH_r^{∞}) is large, yet the relaxation rate is low because the storage temperature is far below the sample's T_g. In contrast, as RH increases and the T_g decreases toward the storage or experiment temperature, the relaxation rate increases and the ΔH_r^{∞} value decreases to zero at T_g (or the fictive temperature, T_f). Finally, at some relative humidity denoted as RH_g, the T_g of the sample equals the experiment temperature. These

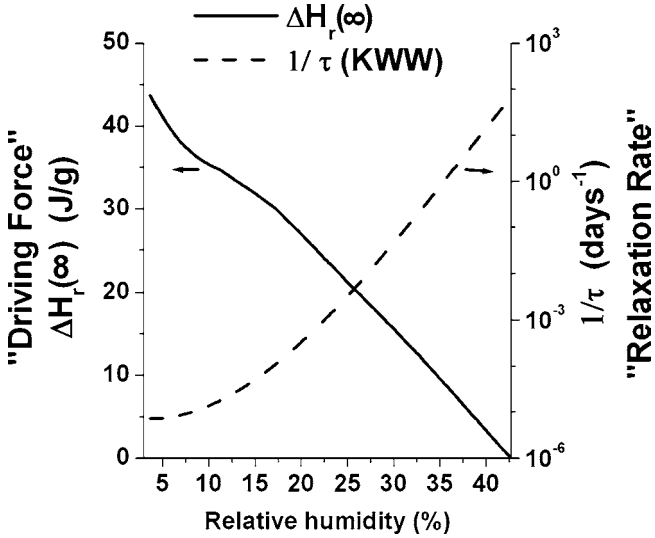

Fig. 9. The rate ($1/\tau$) and driving force (ΔH_r^{∞}) for enthalpy relaxation of spray-dried raffinose as a function of RH (25°C). Relaxation parameters are based upon non-linear least squares fitting of relaxation data to [Eq. (4)]. ΔH_r^{∞} is estimated using Eq. (5). The concepts illustrated in this figure are essential to the understanding of the origin of the take-off point and the associated α-peak.

opposite trends with RH illustrate that, at some intermediate RH, there is a maximum in thermal power due to enthalpy relaxation. Note that, because of the logarithmic scale used to plot the relaxation rate, this maximum is not necessarily located at the intersection of the two curves.

Hodge and Berens (42) simulated the glass transition and enthalpy relaxation response of a given material during a DSC heating scan by treating the heating profile as a series of small temperature steps punctuated by isothermal holding periods [other workers (43) used a finite-element approach]. In an analogous fashion, a continuous RH scan in an RH-perfusion experiment can be envisioned as a series of small RH steps interspersed with (imaginary) observation periods, the duration of each which is related to the RH scan rate. Each step is followed by holding the sample at constant RH for a duration given by:

$$\Delta t = \frac{RH}{\dot{RH}} \tag{7}$$

where $\dot{RH}$ is the linear rate of increase of RH.

To estimate the effect of increasing RH on enthalpy relaxation, we conducted a simulation using the KWW relaxation parameters (τ and β) of raffinose samples equilibrated at discrete temperatures and several moisture contents (see Fig. 8). To model the calorimetric output due to enthalpy relaxation as a function of relative humidity, ΔC_p, and T_g must also be known as a function of RH [see Eq. (5)]. Using Engineering Equation Solver (F-Chart Software, Madison, WI), τ and β values determined from (KWW) analyses of high-sensitivity DSC experiments were fit as a function of RH. The RH-dependences of T_g and ΔC_p were determined from DSC experiments on powder samples pre-equilibrated at several RH values (see Table I). These data were used to estimate the dependence of ΔH_r^∞ on RH using Eq. (5). To simulate the calorimetric power due to enthalpy relaxation as RH is increased in an RH-perfusion experiment, the RH range from 0 to RH_g at 25°C (43% RH) was discretized into ΔRH steps of 1% RH. For a scan rate of 3% RH/h, the duration at each RH step is 0.33 h. Based on values of τ, β, ΔC_p, and T_g as a function of RH, the mean calorimetric power at each RH interval was calculated using Eqs. (3) and (4). These calculations assume that, at each RH step, the fictive temperature of the amorphous material was equal to its T_g. This assumption is unlikely to be accurate at high RH values, conditions under which the T_g of the material approaches the storage temperature. Under such conditions, appreciable enthalpy relaxation occurs over the timescale of the experiment, leading to a complex thermal history (i.e., the fictive temperature continuously decreases in a non-linear fashion during the experiment). In contrast, at RH values near the take-off point, the extent of relaxation is sufficiently small such that this assumption ($T_g = T_f$) is reasonable. Because the location (i.e., the RH value) of the take-off point is most relevant to long-term stability, the uncertainty introduced by a complex thermal history (at higher RH values) is of a lesser practical concern.

Table I. Calorimetric Data of Hydrated Raffinose

RH at 25°C (%)	wt.% H_2O	T_g (°C)	ΔC_p (J g^{-1} K^{-1})
0	0	116	0.58
6.4	2.0	75.2	0.62
11.3	3.0	66.7	0.63
22.5	4.9	49.7	0.66
32.8	6.3	37.8	0.66
43.2	8.7	24.3	ND
52.9	ND	11.6	ND

ND No data.
ΔC_p values are based on the mass of the hydrated sample.
Residual water contents were determined from loss on drying measurements using TGA (collapse of the sample equilibrated at 52.9% RH resulted in incomplete drying in TGA experiments).

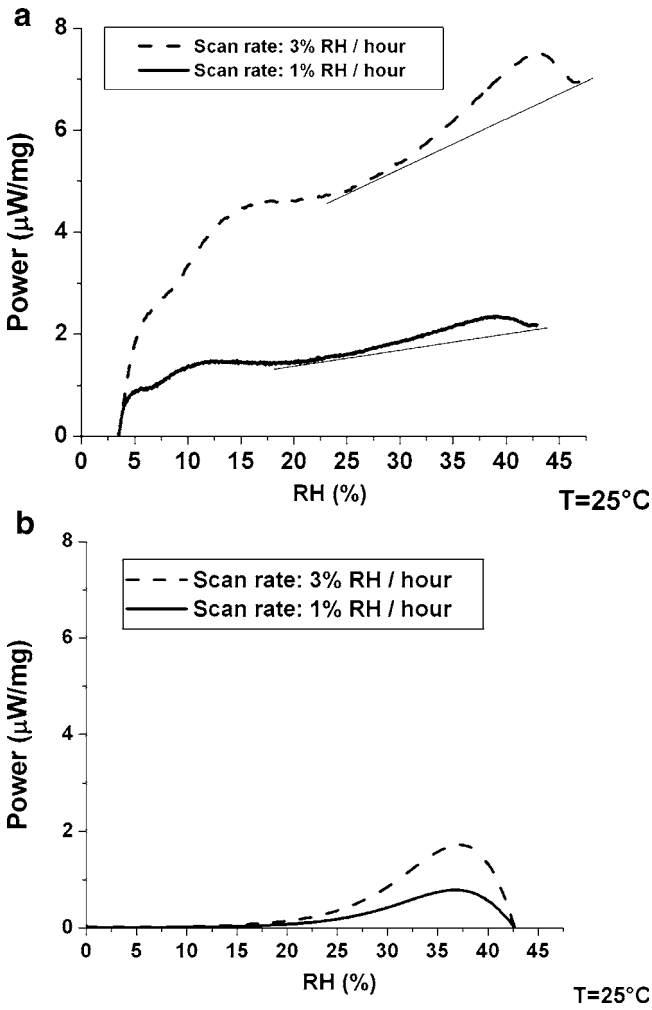

Fig. 10. MITAT of a single spray-dried raffinose for RH scan rates of either 1 or 3% RH/h (25°C): (a) measured MITAT and (b) simulated contribution due to enthalpy relaxation.

Figure 10 shows the comparison between the measured MITAT and the simulated contribution of enthalpy relaxation at two different RH scan rates. The close agreement between the simulated and measured take-off points provides convincing evidence for the origin of the α-peak. The skewness of the α-peak in the MITAT is qualitatively reproduced in the calculated curve. Because the MITAT is the sum of the rates of enthalpy change of all thermal events, it is difficult to quantitatively compare the measured and simulated curves. However, the contribution of moisture

sorption to the thermal power can be estimated by linear extrapolation from the value at the take-off point to that at the end of the α-peak. In this case, given the uncertainty in the estimations of relaxation parameters, the agreement between the order of magnitude of the enthalpies (given by Tthe peak areas) of the measured and simulated results is good. Furthermore, the trend in the simulated calorimetric traces as a function of RH scan rate is consistent with the measured MITAT. Based on these results, we conclude that the α-peak is due to enthalpy relaxation induced by moisture sorption. In principle, using an iterative algorithm of the above simulation, the enthalpy, skewness, and location of this peak could be used to estimate KWW relaxation parameters (τ and β.)

To further investigate the proposed origin of the α-peak, the MITATs of two samples of different "RH history" were measured. The MITAT of a spray-dried raffinose sample was measured during an RH scan from 0 to 36% RH. The sample was aged for almost 24 h at 36% RH and then dried at 0% RH. Following this treatment, the sample remained as discrete particles with no significant change in specific surface area. Because the sample stored at 36% RH was only 9°C below its T_g, it underwent appreciable enthalpy relaxation. After drying for several days at 0% RH, the MITAT of the sample exposed to 36% RH was measured (Fig. 11). Due to the enthalpy relaxation that occurred during storage at 36% RH, the extent of its enthalpy relaxation was less than that of the untreated, initial sample, as evident from the greater (extrapolated) area under the curve of the initial sample. Also, note that the take-off point also shifted to a higher RH value due to enthalpy relaxation during storage at elevated RH; values determined from the 0 and 36% RH samples were about 20 and 33% RH, respectively. The increase in the take-off point of the sample stored at 36% RH reflects the increase in its characteristic relaxation time. This is not unexpected; because the enthalpy relaxation rate depends on the state of the glass, the characteristic relaxation time will increase as structural relaxation proceeds.

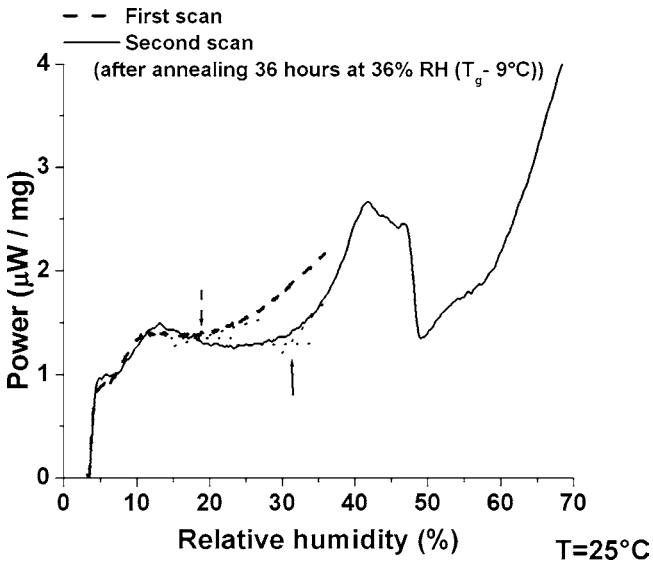

Fig. 11. MITAT of a spray-dried raffinose sample before and after aging for 36 h at 36% RH (25°C), an RH at which T_g = 34°C. *Arrows* indicate RH_m values of original (≈20% RH) and annealed (≈33% RH) samples.

Note that, for a given amorphous solid, the take-off point, RH_m, is not a strictly defined threshold relative humidity. Because enthalpy relaxation occurs at a finite rate at all temperatures below the fictive temperature, the determined value of RH_m will depend on the sensitivity of the calorimeter (or other analytical technique used to assess moisture-induced relaxation). For example, the characteristic relaxation time at the take-off point can be estimated by assuming that the take-off point can be detected as a change above the sorption baseline of 2 μW for a 10 mg sample. Based on values typical for the amorphous solid materials we have studied: β = 0.4, ΔC_p = 0.6 J/g °C, the τ value at the take-off point can be estimated as a function of $T_g - T$ at the take off point based on a rearrangement of Eq. (6) given by:

$$\tau \approx \left(\frac{\Delta C_p \cdot (T_g - T)}{P} \beta t^{\beta-1} \right)^{1/\beta} \qquad (t << \tau) \qquad (8)$$

Figure 12a shows simulated values of τ at RH_m for a few values of β (based on ΔC_p = 0.6 J/g °C). Typically, at the take-off point, the T_g value is between 20 and 40°C above the experimental temperature. For organic glasses that typically have β values near 0.3, these $T_g - T$ values correspond to characteristic relaxation times between 100 days and 4 years, respectively. For the raffinose MITAT at 25°C, RH_m = 20% RH and $T_g - T$ = 53°C−25°C = 28°C. Based on β = 0.3, the estimated characteristic relaxation time from Fig. 12 is about 1 year. Note that the characteristic relaxation time estimated in this manner will be a strong function of the β value. However, when the simulated values are expressed as τ^β as a function of $T_g - T$ (see Fig. 12b), there is a much weaker dependence on β. As discussed previously, the *relative* invariance of τ^β has been reported by Pikal and coworkers. This point is mathematically reflected in Eq. (7), which can be rearranged to give:

$$\tau^\beta \approx \frac{C_p \cdot (T_g - T)}{P} \beta t^{\beta-1} \qquad (t << \tau) \qquad (9)$$

Comparison on the basis of τ^β is preferred not only for its relative invariance (Fig. 12b), but also because it incorporates both the characteristic relaxation time and the width of the distribution of relaxation times. Using Eq. (8) (or Fig. 12b), the τ^β value of a given formulation (with ΔC_p = 0.6 J/g) can be estimated based on the take-off point measured using RH-perfusion calorimetry and the T_g and ΔC_p measured (e.g., using DSC) for a sample equilibrated at the RH of the take-off point. In this manner, the τ^β values of several amorphous formulations can be compared.

Because the β value is related to the distribution of relaxation times, it has an important bearing on molecular mobility. Shamblin *et al.* (44) emphasized that attempts to correlate stability with structural relaxation should consider the distribution of relaxation times. As an example, if the take-off point occurs at $T_g - T$ = 30°C, Fig. 12a shows that characteristic relaxation times could be range from 20 days to more than 1 year for 0.3 < β < 0.5. Thus, without a priori knowledge of β, it is not possible to estimate τ (however, recall that lumped parameter τ^β is relatively invariant for

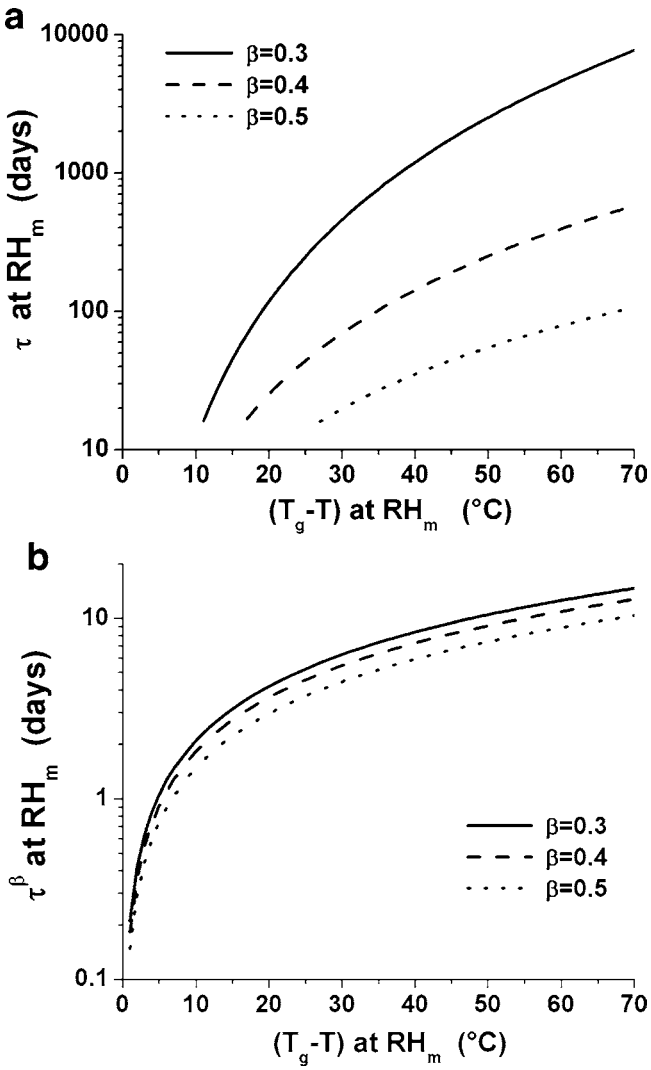

Fig. 12. Estimated characteristic relaxation time at RH_m as a function of the temperature interval below T_g at which RH_m is observed. Results expressed in terms of (a) τ and (b) τ^{β}. Simulations made using Eqs. (8) and (9) (respectively), with $P = 0.2$ μW/mg at the take-off point and $\Delta C_p = 0.6$ J/g °C, and an observation time equivalent to 0.33 h.

typical values of β, see Fig. 12b). One simple approach to estimate β is to first use the procedure outlined by Hancock *et al.* in which the fragility, m, is estimated from the width of the glass transition event, typically measured in a single DSC experiment (26). Then, the fragility can be related to β by the empirical relation proposed by Böhmer *et al.* (39):

$$m = 250 - 320\ \beta \tag{10}$$

It is cautioned that this methodology provides a rough estimate of β. Other, more intensive approaches, such as estimating the fragility from the heating rate dependence of T_g, could lead to better estimates of m and β (26).

The above results show that for instruments (e.g., Thermometric TAM 2277, Setaram Micro DSC III) capable of measuring thermal events on the order of 1 μW, characteristic relaxation times on the order of years can be determined from RH-perfusion experiments. Based on the results shown in Fig. 8, the relaxation time at RH_m increases by several orders of magnitude as the temperature is decreased below T_g. For a DSC scan rate of 10°C/min, the characteristic relaxation time at the calorimetric T_g is reported to be on the order of 400 s (29), though the universality of this value has been debated (45). For a typical pharmaceutical glass ($\beta < 0.3$) with a relaxation time of 400 s at T_g, and a take-off point that occurs at about $T_g - T = 30$°C, the characteristic relaxation time is on the order of years at RH_m, as shown in Fig. 12a. Thus, current instruments are sufficiently sensitive for determination of relaxation times relevant to long-term storage (e.g., 2 years) of amorphous pharmaceutical solids. In the future, additional gains in sensitivity could enable the detection of moisture-induced beta relaxations in proteins and other materials.

To make practical use of estimated relaxation times, it is necessary to consider the relationship between structural relaxation and the processes that lead to physical or chemical instability. A characteristic relaxation time is a measure of molecular mobility. In turn, molecular mobility is related to phenomena involving physical instability, such as viscous flow, collapse, and crystallization. At temperatures below T_g, viscous flow and collapse do not occur to any significant extent. However, crystallization is known to occur at storage temperatures below T_g (46). Though the characteristic time constant for enthalpy (or volume) relaxation might not be equivalent to the time constant for other processes, such as nucleation and crystal growth, their relationship with molecular mobility enables practical use of relaxation times to estimate conditions that are likely to provide long-term physical stability.

Up to this point, this report has focused on determination of enthalpy relaxation as the origin of the sub-T_g thermal event ("α-peak") observed in the MITAT. However, the underlying mechanism for the moisture-induced relaxation remains an open question. Plasticization of amorphous materials by water and other small molecules is a well-known phenomenon. In previous work, we noted the correlation between the water sorption (BET) monolayer and RH_m. Though the BET model has been used to successfully fit moisture sorption isotherm data for many amorphous sys-

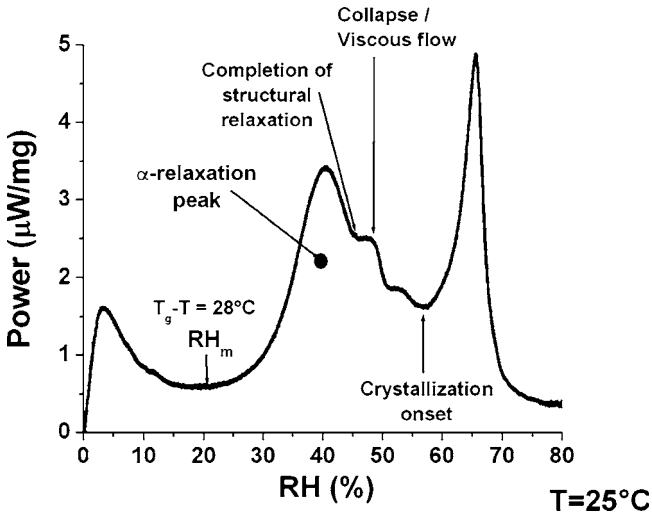

Fig. 13. Annotated events of the moisture-induced thermal activity trace of spray-dried raffinose (25°C).

tems at low-to-moderate RH values, it must be noted that the water sorption monolayer for amorphous systems is not physically well defined because both absorption and adsorption occur (47).

Though there are questions about the physical meaning of a water monolayer for a given amorphous material calculated using the BET and other models, there is undoubtedly a critical moisture content below which long-term stability is observed. One explanation is that an amorphous solid contains a finite amount of hydrophilic sites that become saturated at some critical moisture content. Above this moisture content, ad/absorbed water molecules have a greater molecular mobility. Thus, water exhibits different behavior below and above this critical moisture content. This water-binding site saturation hypothesis is supported by calorimetric measurements that show that, above RH_m, the heat of water sorption approaches the enthalpy of condensation of water.

Regardless of the underlying mechanism, the correlation of RH_m with long-term physical stability has practical value. This work demonstrates the utility of RH-perfusion calorimetry at providing a rapid, straightforward technique to estimate the combined effect of temperature and RH on the stability of amorphous solids. The ability to compare formulations based on molecular mobility below T_g provides significant advantages over formulation screening based on T_g alone. Furthermore, RH perfusion experiments conducted on a material at several temperatures provides a means to prepare a long-term stability diagram that is useful for determining RH and temperature conditions that ensure stability of pharmaceutical materials during processing, handling, and use. Such diagrams will be the subject of a forthcoming research article.

CONCLUSIONS

RH-perfusion microcalorimetry can be considered as the relative humidity analog of differential scanning calorimetry; instead of the thermal response of an imposed temperature profile, RH-perfusion calorimetry provides a measure of the thermal response to a programmed relative humidity profile. This technique provides a rapid measure of the interactions between water vapor and amorphous pharmaceutical solids. The resulting calorimetric trace, known as the moisture induced isothermal activity trace (MITAT), shows general behavior for many amorphous pharmaceutical solids. At some relative humidity threshold, RH_m, the MITAT exhibits a substantial increase in the calorimetric power, which is proportional to the rate of heat production. Below this RH value, long-term physical stability (i.e., on the order of years) is observed. Our observations, reinforced with literature data demonstrating long-term physical stability, provide support for RH_m as a meaningful indicator of long-term physical, and perhaps chemical, stability.

Because of the non-specific nature of calorimetry, multiple solid-state characterization techniques were used to further interpret and understand the origin of thermal events comprising the MITAT of a model amorphous material. The calorimetric events in the moisture-induced thermal activity trace of spray-dried raffinose (25°C) have been annotated in Fig. 13. Macroscopically detectable events such as collapse and crystallization were determined using X-ray powder diffraction and gravimetric vapor sorption. Though the take-off point was not found to be associated with a sudden increase in the rate of moisture sorption, analysis of derivative gravimetric moisture uptake data did provide a useful means to detect the RH that leads to macroscopic structural collapse of an amorphous material. Other events, such as recrystallization, could also be assessed using both calorimetric and (derivative) gravimetric techniques.

Because of its relevance to long-term stability, understanding the take-off point was the primary objective of this work. Isothermal enthalpy relaxation measurements (using high-sensitivity differential scanning calorimetry) on hydrated samples of fixed composition were used as inputs to a mathematical simulation of enthalpy relaxation induced by moisture uptake. This model correctly predicted the take-off point and was able to explain the shape of the subsequent peak in thermal activity. These results indicated that the origin of the take-off point is the onset of detectable enthalpy relaxation. The mechanistic understanding of these observations adds further value to the use of RH-perfusion calorimetry as a rapid means to characterize the molecular mobility of amorphous solids. Further modeling work showed that commercially available microcalorimeters are able to determine relaxation times relevant to long-term storage of amorphous pharmaceutical solids.

Though the underlying molecular-level mechanism for moisture-induced relaxation remains an open question, RH perfusion calorimetry still has considerable practical value. The ability to compare formulations on the basis of molecular mobility at temperatures below T_g provides significant advantages over formulation screening based on T_g alone or based on rules of thumb, such as recommending a storage temperature at least 50 K below T_g. RH-perfusion calorimetry measurements at several temperatures provide a means to estimate the combined effect of temperature and RH on the stability of amorphous solids. Most remarkably, thermal events measured on practical laboratory timescales (hours to days) are relevant to the stability of amorphous materials on much longer, pharmaceutically relevant timescales (years).

ACKNOWLEDGMENTS

The authors gratefully acknowledge our colleagues from Nektar Therapeutics for helpful discussions and insight provided throughout the course of this work.

REFERENCES

1. G. Van den Mooter, P. Augustijns, and R. Kinget. Stability prediction of amorphous benzodiazepines by calculation of the mean relaxation time constant using the Williams–Watts decay function. *Eur. J. Pharm. Biopharm.* **48**(1):43–48 (1999).
2. S. P. Duddu, G. Zhang, and P. R. Dal Monte. The relationship between protein aggregation and molecular mobility below the glass transition temperature of lyophilized formulations containing a monoclonal antibody. *Pharm. Res.* **14**(5):596–600 (1997).
3. R. A. Shmeis, Z. Wang, and S. L. Krill. A mechanistic investigation of an amorphous pharmaceutical and its solid dispersions, part I: A comparative analysis by thermally stimulated depolarization current and differential scanning calorimetry. *Pharm. Res.* **21**:2025–2030 (2004).

4. S. Yoshioka, S. Tajima, Y. Aso, and S. Kojima. Inactivation and aggregation of beta-galactosidase in lyophilized formulation described by Kohlrausch–Williams–Watts stretched exponential function. *Pharm. Res.* **20**(10):1655–1660 (2003).
5. J. Liu, D. R. Rigsbee, C. Stotz, and M. J. Pikal. Dynamics of pharmaceutical amorphous solids: the study of enthalpy relaxation by isothermal microcalorimetry. *J. Pharm. Sci.* **91**:1853–1862 (2002).
6. V. Andronis and G. Zografi. The molecular mobility of supercooled amorphous indomethacin as a function of temperature and relative humidity. *Pharm. Res.* **15**(6):835–842 (1998).
7. S. P. Duddu and T. D. Sokoloski. Dielectric analysis in the characterization of amorphous pharmaceutical solids. 1. Molecular mobility in poly(vinylpyrrolidone)—water systems in the glassy state. *J. Pharm. Sci.* **84**:773–776 (1995).
8. S. Yoshioka, Y. Aso, and S. Kojima. Temperature- and glass transition temperature-dependence of bimolecular reaction rates in lyophilized formulations described by the Adam–Gibbs–Vogel equation. *J. Pharm. Sci.* **93**(4):1062–1069 (2004).
9. H. Hu and C. T. Sun. The equivalence of moisture and temperature in physical aging of polymeric composites. *J. Compos. Mater.* **37**:913–928 (2003).
10. B. Borde, H. Bizot, G. Vigier, and A. Buléon. Calorimetric analysis of the structural relaxation in partially hydrated amorphous polysaccharides. I. Glass transition and fragility. *Carbohydr. Polym.* **48**:83–96 (2002).
11. D. Lechuga-Ballesteros, A. Bakri, and D. P. Miller. Microcalorimetric measurement of the interactions between water vapor and amorphous pharmaceutical solids. *Pharm. Res.* **20**(2):308–318 (2003).
12. B. Makower and W. B. Dye. Equilibrium moisture content and crystallization of amorphous sucrose and glucose. *J. Agric. Food Chem.* **4**:72–77 (1956).
13. H. Binder, B. Kohlstrunk, and H. H. Heerklotz. Hydration and lyotropic melting of amphiphilic molecules: A thermodynamic study using humidity titration calorimetry. *J. Colloid Interface Sci.* **220**(2):235–249 (1999).
14. V. P. Lehto and E. Laine. Simultaneous determination of the heat and the quantity of vapor sorption using a novel microcalorimetric method. *Pharm. Res.* **6**:701–706 (2000).
15. M. Pudipeddi, T. D. Sokoloski, S. P. Duddu, and J. T. Carstensen. Quantitative characterization of adsorption isotherms using isothermal microcalorimetry. *J. Pharm. Sci.* **85**(4):381–386 (1996).
16. L. Greenspan. Humidity fixed points of binary saturated aqueous solutions. *J. Res. Natl. Bur. Stand. Sec., A* **81**:89–102 (1977).
17. A. Bakri. Design, testing and pharmaceutical applications of a gas pressure controller device for solid-gas microcalorimetric titration. In *ThermoMetric Application Note 22021*, Thermometric AB, Sweden, 4 (1993).
18. K. Chatterjee, E. Y. Shalaev, and R. Suryanarayanan. Partially crystalline systems in lyophilization: I. Use of ternary state diagrams to determine extent of crystallization of bulking agent. *J. Pharm. Sci.* **94**(4):798–808 (2005).
19. K. Kajiwara, F. Franks, P. Echlin, and A. L. Greer. Structural and dynamic properties of crystalline and amorphous phases in raffinose-water mixtures. *Pharm. Res.* **16**:1441–1448 (1999).
20. A. Saleki-Gerhardt, J. G. Stowell, S. R. Byrn, and G. Zografi. Hydration and dehydration of crystalline and amorphous forms of raffinose. *J. Pharm. Sci.* **84**(3):318–323 (1995).
21. G. E. Downton, J. L. Flores-Luna, and C. J. King. Mechanism of stickiness in hygroscopic, amorphous powders. *Ind. Eng. Chem. Fundam.* **21**:447–451 (1982).
22. M. E. Lazar, A. H. Brown, G. S. Smith, F. F. Wong, and F. E. Lindquist. Experimental production of tomato powder by spray drying. *Food Technol.* **3**:129–134 (1956).
23. D. A. Wallack and C. J. King. Sticking and agglomeration of hygroscopic amorphous carbohydrate and food powders. *Biotechnol. Prog.* **4**(1):31–35 (1988).
24. Y. Frenkel. Viscous flow of crystalline bodies under the action of surface tension. *J. Phys. (USSR)* **9**(5):385–391 (1945).
25. M. Peleg and C. H. Mannheim. The mechanism of caking of powdered onion. *J. Food Process. Preserv.* **1**:3–11 (1977).
26. B. C. Hancock, C. R. Dalton, M. J. Pikal, and S. L. Shamblin. A pragmatic test of a simple calorimetric method for determining the fragility of some amorphous pharmaceutical materials. *Pharm. Res.* **15**(5):762–767 (1998).
27. I. M. Hodge. Adam–Gibbs formulation of enthalpy relaxation near the glass transition. *J. Res. Natl. Inst. Sci. Technol.* **102**:195–205 (1997).
28. C. A. Angell, K. L. Ngai, G. B. McKenna, P. F. McMillan, and S. W. Martin. Relaxation in glassforming liquids and amorphous solids. *J. Appl. Phys.* **88**:3113–3157 (2000).
29. C. T. Moynihan. Structural relaxation and the glass transition. *Rev. Miner.* **32**:1–19 (1995).
30. L. C. E. Struik. *Physical Aging in Amorphous Polymers and other Materials*, Elsevier, Amsterdam, 1978.
31. A. Q. Tool. Relations between inelastic deformability and thermal expansion of glass in its annealing range. *J. Am. Ceram. Soc.* **29**:240 (1946).
32. O. S. Narayanaswamy. A model of structural relaxation in glass. *J. Am. Ceram. Soc.* **54**(10):491 (1971).
33. G. B. McKenna. On the physics required for the prediction of long-term performance of polymers and their composites. *J. Res. Natl. Inst. Stand. Technol.* **99**:169–189 (1994).
34. F. Kohlrausch. *Pogg. Ann. Phys.* **199**:352 (1863).
35. G. Williams and D. C. Watts. Non-symmetrical dielectric relaxation behavior arising from a simple decay function. *Trans. Faraday Soc.* **66**:80–85 (1970).
36. J. M. G. Cowie, S. Harris, and I. J. McEwen. Physical aging in poly(vinyl acetate) 2. Relative rates of volume and enthalpy relaxation.. *Macromolecules* **31**:2611–2615 (1998).
37. B. C. Hancock, S. L. Shamblin, and G. Zografi. The molecular mobility of amorphous pharmaceutical solids below their glass transition temperatures. *Pharm. Res.* **12**(6):799–806 (1995).
38. S. Yoshioka, Y. Aso, and S. Kojima. Usefulness of the Kohlrausch–Williams–Watts stretched exponential function to describe protein aggregation in lyophilized formulations and the temperature dependence near the glass transition temperature. *Pharm. Res.* **18**(3):256–260 (2001).
39. R. Böhmer, K. L. Ngai, C. A. Angell, and D. J. Plazek. Nonexponential relaxations in strong and fragile glass-formers. *J. Chem. Phys.* **99**(5):4201–4209 (1993).
40. H. L. Hampsch, J. Yang, G. K. Wong, and J. M. Torkelson. *Macromolecules* **23**:3640–3647 (1990).
41. K. Kawakami and M. J. Pikal. Calorimetric investigation of the structural relaxation of amorphous materials: evaluating validity of the methodologies. *J. Pharm. Sci.* **94**(5):948–965 (2005).
42. I. M. Hodge and A. R. Berens. Effects of annealing and prior history on enthalpy relaxation in glassy polymers 2. Mathematical modeling. *Macromolecules* **15**:762–770 (1982).
43. J. N. Hay and M. J. Jenkins. Simulation of the glass transition. *J. Therm. Anal. Calorim.* **56**:1005–1010 (1999).
44. S. L. Shamblin, B. C. Hancock, Y. Dupuis, and M. J. Pikal. Interpretation of relaxation time constants for amorphous pharmaceutical systems. *J. Pharm. Sci.* **89**(3):417–427 (2000).
45. D. J. Plazek and C. A. Bero. Precise glass temperatures. *J. Phys., Condens. Matter* **15**:S789–S802 (2003).
46. M. Yoshioka, B. C. Hancock, and G. Zografi. Crystallization of indomethacin from the amorphous state below and above its glass transition temperature. *J. Pharm. Sci.* **83**(12):1700–1705 (1994).
47. J. T. Carstensen and K. Van Scoik. Amorphous-to-crystalline transformation of sucrose. *Pharm. Res.* **7**(12):1278–1281 (1990).